

Evaluating Protein Attraction and Adhesion to Biomaterials with the Atomic Force Microscope

Min Sze Wang, Laura B. Palmer, Jay D. Schwartz, and Anneta Razatos*

Department of Chemical and Materials Engineering, Arizona State University,
Tempe, Arizona 85287-6006

Received January 16, 2004. In Final Form: June 2, 2004

Failure of implanted biomaterials is commonly due to nonspecific protein adsorption, which in turn causes adverse reactions such as the formation of fibrous capsules, blood clots, or bacterial biofilm infections.¹ Current research efforts have focused on modifying the biomaterial interface to control protein reactions. Designing biomaterial interfaces at the molecular level, however, requires an experimental technique that provides detailed, dynamic information on the forces involved in protein adhesion. The goal of this study was to develop an atomic force microscope (AFM)-based technique to evaluate protein adhesion on biomaterial surfaces. In this study, the AFM was used to evaluate (i) protein–protein, (ii) protein–substrate, and (iii) protein–dextran interactions. The AFM was first used to measure the pull-off forces between bovine serum albumin (BSA) tips/BSA surfaces and BSA tips/anti-BSA surfaces. Results from these protein–protein studies were consistent with the literature. More importantly, the successful measurement of antibody–antigen binding interactions demonstrates that both the BSA and anti-BSA proteins retain their folded conformation and remain functional following our immobilization protocol. The AFM was also used to quantify the physiochemical interactions of proteins during adhesion to various self-assembled monolayers (SAMs) and dextran-coated substrates representative of potential biomaterial interface modifications. Dextran, which renders surfaces very hydrophilic, was the only surface coating that BSA protein did not adhere to. Hydrophobic interactions were not found to play a significant role in BSA adhesion. Therefore, the dextran molecules may resist protein adhesion by repulsive steric effects or hydration pressure. Moreover, the AFM-based methodology provides dynamic, quantitative information about protein adhesion at the nanoscale level.

Introduction

Immediately upon implantation, biomaterial substrates become coated with serum or plasma proteins such as albumin, IgG, and fibrinogen.^{2–7} Albumin, the most abundant protein, adsorbs first but is displaced by larger proteins that interact more favorably with the underlying substrate, a process known as the Vroman effect.² These adsorbed proteins are unable to maintain their native structures and in turn will cause adverse reactions such as the formation of fibrous capsules adjacent to soft tissue implants or blood clots inside synthetic vascular grafts.¹ Protein fouling of biomaterials also renders biomaterials susceptible to colonization and infection by bacteria.^{4,7–9}

Until recently, the adsorption and accumulation of biological material on implanted biomaterial surfaces have been irreversible and uncontrollable.¹⁰ Recent advances in biomaterial design, however, have reduced undesirable

protein adsorption and unfavorable cell adhesion onto the materials. Biomaterial development has focused on creating adhesion-resistant interfaces as a solution to protein fouling, bacterial infections, and adverse physiological reactions. Most protein-resistant polymeric biomaterials and coatings include poly(ethylene glycol) (PEG), poly(ethylene oxide) (PEO), and their derivatives.^{10,11} An alternative material to PEG is dextran. Recent studies show that dextran-coated biomaterial surfaces provide low protein binding and anticellular adhesion comparable to PEG.¹² The advantage to using dextran-coated surfaces is that dextran provides multiple reactive sites for immobilization of biologically active molecules.¹² Therefore, dextran coatings can provide low protein binding with functional biological molecules.

In the development of protein-resistant interfaces, nonspecific protein adhesion is evaluated by experimental techniques such as mass spectroscopy, X-ray photoelectron spectroscopy (XPS), surface plasmon resonance (SPR), and secondary-ion mass spectrometry (SIMS). Although valuable at quantifying the amount and types of proteins adsorbed on biomaterials, these techniques do not provide information on the physiochemical interactions involved in adhesion. Moreover, they do not differentiate between long-range attractive/repulsive interaction and short-range binding events. The current push to design biomaterial interfaces at the molecular level requires an experimental technique that provides detailed, dynamic information on the forces driving protein adhesion.

The goal of this study was to develop an atomic force microscope (AFM)-based methodology to evaluate protein

* Corresponding author. Current address: Department of Chemical Engineering, Arizona State University, P.O. Box 876006, Tempe, AZ 85287-6006. E-mail: razatos@asu.edu. Phone: 480-965-0874. Fax: 480-965-0037.

(1) Caster, D. G.; Ratner, B. D. *Surf. Sci.* **2002**, *500*, 28–60.
(2) Vroman, L.; Adams, A.; Fisher, G.; Munoz, P. *Blood* **1980**, *55*, 156–159.
(3) Yu, J. L.; Ljungh, A.; Andersson, R.; Jakab, E.; Bengmark, S.; Wadström, T. *J. Med. Microbiol.* **1994**, *41*, 133–138.
(4) Gristina, A. G. *Science* **1987**, *237*, 1588–1595.
(5) Green, R.; Davies, J.; Davies, M.; Roberts, C.; Tendler, S. *Biomaterials* **1997**, *18*, 405–413.
(6) Santin, M.; Motta, A.; Denyer, S.; Cannas, M. *Biomaterials* **1999**, *20*, 1245–1251.
(7) Stickler, D. J.; McLean, R. J. C. *Cells Mater.* **1995**, *5*, 167–182.
(8) Reid, G. *Colloids Surf., B* **1994**, *2*, 377–385.
(9) Costerton, J. W.; Stewart, P. S.; Greenberg, E. P. *Science* **1999**, *284*, 1318–1322.
(10) Kingshott, P.; Griesser, H. J. *Curr. Opin. Solid State Mater. Sci.* **1999**, *4*.

(11) Massia, S. P.; Letbetter, D. S.; Stark, J. *Biomaterials* **2000**, *21*, 2253–2261.

(12) Massia, S. P.; Stark, J. *J. Biomed. Mater. Res.* **2001**, *56*, 390–399.

adhesion on biomaterials. The advantage to using this technique is that the AFM provides quantitative information on the magnitude and nature of the underlying forces driving protein adhesion. Results from these studies are quantitative (force vs distance curves), reproducible, and can be analyzed/ modeled according to colloid theory. In this study, the AFM was used to evaluate (i) protein–protein, (ii) protein–substrate, and (iii) protein–dextran interactions. Results from this study demonstrate that the AFM provides detailed information on protein attraction and adhesion to inanimate and biological systems in solution. Using the AFM with other protein-adhesion techniques will provide a complete understanding of protein–substrate interactions.

Materials and Methods

Preparation of Gold Surfaces. Silicon wafers (WaferNet, San José, CA) and Si_3N_4 cantilevers (Veeco Digital Instruments, Santa Barbara, CA) were cleaned in a piranha etching solution of 70 vol % sulfuric acid to 30 vol % hydrogen peroxide (Mallinckrodt, Paris, KY) for 30 min. The cleaned silicon wafers and cantilevers were then rinsed with copious distilled, deionized (DI) water (Millipore Elix S, Bedford, MA) and dried in a 120 °C oven for 2 h. The wafers and cantilevers were first coated with 10 Å of chrome, immediately followed by 250 Å of gold (99.999%, Alfa Aesar, Ward Hill, MA) in an Edwards Auto 306 high-vacuum evaporator (ASU Center for Solid State Electronic Research, Tempe, AZ). The system is equipped with a diffusion pump with a liquid nitrogen trap and was operated at a base pressure of 10^{-6} Torr.

Preparation of Self-Assembled Monolayers (SAMs) on Gold-Coated Surfaces. SAMs of 1-mercaptohexadecane ($\text{HS}(\text{CH}_2)_{16}\text{CH}_3$), 16-mercaptohexadecanol ($\text{HS}(\text{CH}_2)_{16}\text{OH}$), and 16-mercaptohexadecanoic acid ($\text{HS}(\text{CH}_2)_{16}\text{COOH}$) were purchased from Aldrich (Aldrich, St. Louis, MO) and were diluted to 1 mM solutions in 50% aqueous ethanol (200 proof, AAPER, Shelbyville, KY). Gold-coated wafers and cantilevers (250 Å) were immersed into each of the 1 mM SAM solutions and incubated at 37 °C in dark conditions. After the incubation period, the wafers and cantilevers were rinsed thoroughly with ethanol and dried under nitrogen. Methyl and hydroxyl terminated SAMs were prepared as described above. Dextran immobilized on gold-coated silicon wafers (1000 Å) was kindly provided by Professor Stephen Massia (Department of Bioengineering, Arizona State University).

Protein Immobilization on SAM Functionalized Surfaces. A 9.58 mL portion of *N,N*-dimethyl formamide (*N,N*-DMF, anhydrous, Aldrich, St. Louis, MO), 0.28 mL of triethylamine (99.5%, Aldrich, St. Louis, MO), and 0.14 mL of trifluoroacetic anhydride (99+%, Aldrich, St. Louis, MO) were added in that order to a 20 mL vial. The wafers and cantilevers were added to the vials and were incubated at room temperature for 20 min. The wafers and cantilevers were thoroughly rinsed with dichloromethane (Mallinckrodt, Paris, KY) and dried under nitrogen. Immediately following nitrogen drying, the wafers and cantilevers were immersed in a 5 mg/mL protein (Aldrich, St. Louis, MO) in PBS (phosphate buffered saline, pH 7.4) solution for 30 min at room temperature. The wafers and cantilevers were then rinsed with water and dried under nitrogen. Bovine serum albumin (BSA) (Sigma Aldrich, St. Louis, MO) and anti-BSA (Sigma Aldrich, St. Louis) were immobilized on cantilevers and silicon wafers, respectively. Figure 1 illustrates a schematic representation of a covalently immobilized BSA molecule on an AFM tip.

AFM Force Measurements and Data Analysis. Protein–substrate and protein–protein forces were measured with a NanoScope E MultiMode AFM (Digital Instruments, Santa Barbara, CA). The cantilevers used in this study had the following dimensions: length = 194 μm , width = 21 μm , and thickness = 0.44 μm (Digital Instruments, Santa Barbara, CA). Force measurements were performed in a standard AFM fluid cell filled with 10 mM PBS (pH 7.4) buffer at room temperature. The AFM was operated for a Z-scan size of 100 nm and a scan rate of 4.00 Hz. The process was repeated at least three times for each tip/surface combination.

AFM data were reported in terms of tip deflection versus the relative distance of separation. The data were converted to force

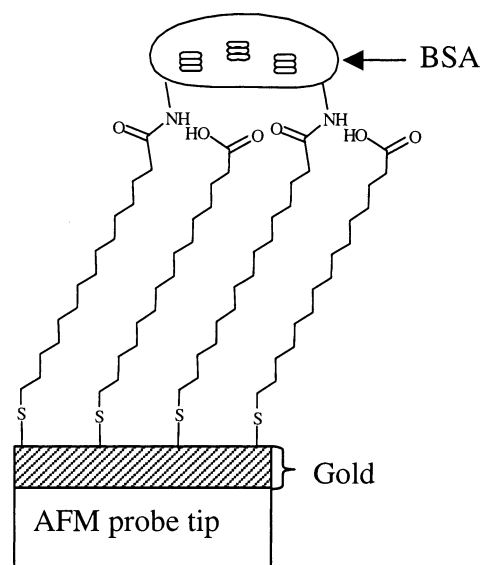


Figure 1. Schematic representation of a covalently attached BSA molecule on an AFM cantilever tip.

(nanonewtons) versus the absolute distance of separation (nanometers) by treating the cantilever as a spring with a characteristic spring constant (k) according to Hooke's law: $F = -k\Delta Y$, where ΔY is the tip deflection. In this study, the point of contact between the cantilever and the substrate was assumed to occur at the lowest point of the extending curve. In other words, the lowest point was taken as the point of contact, also known as the zero distance of separation. When quantifying the pull-off force, the tip deflection (ΔY) was calculated as the difference between the flat portion and the lowest point of the retraction curve (the point where the tip breaks contact with the sample surface).

Spring Constant Measurement. Spring constants (k values) of the bare and modified AFM cantilevers were measured using a tapping mode AFM (Nanoscope IIIa controller with a PicoForce modulator; Digital Instruments, Santa Barbara, CA). The measurements were performed in air over a piece of freshly cleaved mica substrate at room temperature (25 °C). The 200 μm V-shaped cantilevers were used throughout the measurement. Spring constant data were obtained from the Nanoscope (version 6) software that provides a fully automated cantilever spring constant calibration. The spring constants of 10 cantilevers were measured for bare Si_3N_4 , 250 Å gold-coated and BSA-coated cantilevers.

Fourier Transform Infrared Spectroscopy. Infrared spectra were collected with a Thermo Nicolet 470 spectrometer (Thermo Nicolet, Madison, WI) with a liquid nitrogen cooled mercury cadmium telluride (MCT) detector. The sample chamber was purged with nitrogen to remove water and carbon dioxide. A Thermo Nicolet smart apertured grazing angle (SAGA) accessory with a grazing angle of incidence of 80° was used to collect reflection absorption infrared spectroscopy (RAIRS) spectra. The resolution was set to 2 cm^{-1} and 1024 scans were collected.

Contact Angle Measurements. Contact angles were measured using a Ramé-Hart standard automated goniometer (model 200-00) at room temperature and ambient humidity. A sessile drop of either water or PBS (pH 7.4) was placed on the surface using a manual syringe fixture. Upon contact with the surface, the sessile drop advanced over the surface. The advancing contact angles were measured within 20 s following contact.

Results

The AFM was used in this study to quantify the physiochemical interactions of proteins during adhesion to various substrates. Measurements involved immobilizing proteins on tips of AFM cantilevers, which were then used to probe substrates of interest in physiological buffer. Proteins were immobilized in random orientations directly on the tips of standard AFM cantilevers similar to the

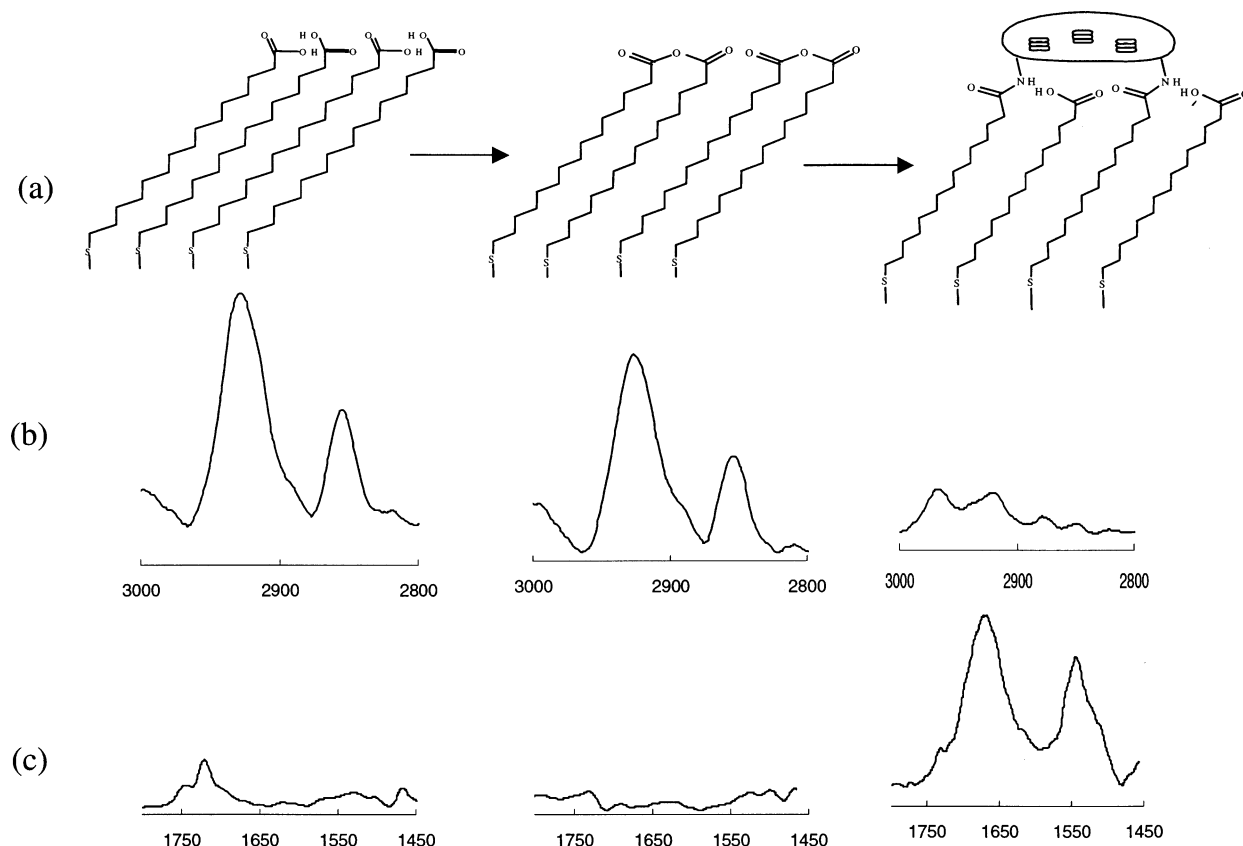


Figure 2. RAIRS spectra of a BSA-coated surface demonstrating each major step of the immobilization technique. Part a shows the molecular structure of the SAMs and BSA protein. Part b shows the asymmetric and symmetric stretches of the CH group of SAMs in the 2800–3000 cm⁻¹ region. Part c shows the C=O and N–H stretches of BSA protein in the 1400–1700 cm⁻¹ region.

protocol of Yan et al.¹³ Bovine serum albumin (BSA) protein was chosen for this proof-of-concept study because adhesion of this protein has been extensively studied. Protein–protein interactions were measured as a control to demonstrate the integrity of the immobilization protocol. Specifically, the AFM was used to measure the pull-off forces between BSA tips/BSA surfaces and BSA tips/anti-BSA surfaces. BSA-protein-coated tips were then used to probe model (SAM) substrates and dextran-coated substrates representative of potential biomaterial interfaces.

SAMs represent a simple, reproducible and effective method of modifying surfaces in order to change their chemical and physicochemical properties. There has been a tremendous increase in the use of SAMs to coat or modify biomaterials (especially metal oxides) because SAMs are clean, uniform, and stable.¹⁴ SAM substrates are ideal for AFM studies because they are smooth, structurally ordered, and chemically defined at the microscopic scale.¹⁴ The most extensively studied SAM substrate system has been alkanethiols on gold, where the thiols react readily with gold surfaces to create uniform monolayers.¹⁵ In this study, methyl terminated alkanethiols (1-mercaptohexadecane) were used to prepare a hydrophobic interface, whereas hydroxyl terminated molecules (16-mercaptohexadecanol) formed a hydrophilic interface. Amine terminated SAMs were also evaluated because they are commonly used as a precursor to immobilizing biological molecules (such as dextran, proteins, or peptides) to

biomaterials. Dextran covalently immobilized on gold-coated silicon wafers also represents a promising technology of modifying biomaterial interfaces in order to reduce protein adhesion and unfavorable physiological responses. The AFM was used in this study to evaluate protein–SAM substrate interactions. The AFM measured both the affinity and attraction that a protein in solution has for a substrate and the strength of protein binding during adhesion.

Characterization of SAMs and Protein Immobilization by FTIR. The chemical and physical properties of the SAMs and the protein immobilization protocol were determined at each step of their preparation by FTIR. FTIR spectroscopy was used to verify the presence and packing of the following SAMs on gold: (a) methyl, (b) hydroxyl, (c) carboxylic acid, (d) amine terminated, and (e) dextran. In all cases, the symmetric and asymmetric stretches of –CH₂– occurred at 2925 and 2852 cm⁻¹, respectively, which is consistent with the literature¹⁶ (data not shown). Likewise, for the CH₃– vibrations, the symmetric peaks appeared at 2962 cm⁻¹ and the asymmetric peaks at 2881 cm⁻¹ (data not shown). The FTIR results on SAMs confirmed proper preparation and packing of the molecules on the metal oxide surface.

Proteins were immobilized onto SAM-modified silicon wafers and AFM cantilevers on the basis of the work of Yan et al.¹³ In brief, a self-assembled monolayer of a carboxylic acid terminated SAM (16-mercaptohexadecanoic acid) was formed on the gold surface. The carboxylic acid terminus was then converted to a reactive interchain anhydride with trifluoroacetic anhydride. This interchain anhydride reacts with free amine groups of proteins to

(13) Yan, L.; Marzolin, C.; Terfort, A.; Whitesides, G. M. *Langmuir* **1997**, *13*, 6704–6712.

(14) Tosatti, S.; Michel, R.; Textor, M.; Spencer, N. D. *Langmuir* **2002**, *18*, 3537–3548.

(15) Hofer, R.; Textor, M.; Spencer, N. D. *Langmuir* **2001**, *17*, 4014–4020.

(16) Bertilsson, L.; Liedberg, B. *Langmuir* **1993**, *9*, 141–149.

Table 1. Infrared Frequencies and Assignments of Proteins Covalently Attached to the AFM Cantilever Tips

assignment	description	frequency (cm ⁻¹)	
		BSA	anti-BSA
ν (C=O)	amide I, C=O stretch	1669	1661
ν (C-N)	amide II, N-H bend and C-H stretch	1539	1537

Table 2. Advancing Contact Angle Measurements of CH₃, OH, COOH, and NH₂ Terminated SAMs, Dextran, and BSA with Water and PBS

surface	contact angle (deg)		surface	contact angle (deg)	
	water	PBS		water	PBS
CH ₃	117.4 ± 0.2	117.0 ± 0.4	NH ₂	73.2 ± 0.6	78.1 ± 0.7
OH	82.4 ± 0.6	85.9 ± 0.8	dextran	41.2 ± 0.6	46.3 ± 1.6
COOH	72.1 ± 0.3	78.7 ± 1.3	BSA	55.9 ± 1.3	53.2 ± 0.7

form a covalent bond. Free amines include the amino terminus and any of the lysine residues of BSA resulting in random orientation of the protein. Figure 2 summarizes the chemistry and corresponding RAIRS spectra for each of the formation steps in the immobilization protocol.

BSA and anti-BSA proteins immobilized onto the SAM-modified silicon wafers were characterized by grazing angle FTIR with an 80° angle of incidence. The FTIR spectra of covalently immobilized BSA and anti-BSA are summarized in Table 1. The most prominent peaks of the amide groups of proteins were located at ~1665 and ~1539 cm⁻¹. These peaks correspond to the C=O stretch (1600–1700 cm⁻¹) and the N-H bend plus the C-N stretch (1510–1580 cm⁻¹). The FTIR results demonstrate the successful immobilization of proteins on the SAM substrate.

Contact Angle Measurements of Substrates. The surface hydrophobicity of the SAM substrates was determined by sessile drop contact angle measurements. Information on the surface properties of the substrates is necessary for the analysis of AFM force measurements in the context of colloid theory. The advancing contact angle was measured in air with either distilled, deionized water or PBS buffer (Table 2). By convention, contact angles are evaluated in water; however, our AFM force measurements were performed in PBS buffer. Therefore, the contact angle measurements were performed in both solutions to determine if the PBS buffer altered the surface properties of the SAM substrates. There were no significant differences between the contact angles measured in water versus PBS (Table 2).

Larger contact angles indicate a more hydrophobic surface. As expected, the methyl (CH₃) terminated SAMs had the largest contact angle of 117°, indicating that this surface was the most hydrophobic. The hydroxyl (OH) terminated SAMs were hydrophilic with contact angles of 82° but not as hydrophilic as the carboxylic acid and amine terminated SAMs. Both the carboxylic acid (COOH) and amine (NH₂) terminated SAMs were hydrophilic, with contact angles of 72 and 73°, respectively. The most hydrophilic surface was dextran, with the smallest contact angle of 41°. As expected, surfaces became hydrophilic when they were coated with BSA proteins; the contact angle of the BSA-coated gold substrates was 53°.

Spring Constant Calibration. The AFM is a powerful tool for investigating surface properties at the atomic level. It measures forces and provides topographical information in contact mode. In noncontact mode, the AFM operates by scanning over the sample surface with a resonating cantilever that moves close to the sample. The resonant

frequency of the cantilever changes due to the force gradient between the tip and the sample. This change in resonant frequency causes the spring constant to change.¹⁷ In tapping mode, the sample surface is scanned at a constant vibration amplitude or resonance frequency. Using a closed-loop feedback circuit, the tip/sample position is adjusted to the change in the root-mean-square (rms) amplitude of the cantilever vibration.

A number of methods for determining the spring constant have been proposed. For example, Cleveland et al. determined the spring constant by measuring the change in resonant frequency with added end mass to the cantilever;^{18,19} Hutter and Bechhoefer demonstrated that the spring constant may be determined by the measurement of thermal noise in the cantilever,¹⁹ and Senden and Ducker used the static deflection of a cantilever under the force of a known end mass to determine the spring constant.²⁰ In this study, we used the Digital Instruments MultiMode PicoForce AFM with the Nanoscope (version 6) software to calibrate our AFM cantilever spring constants. Measurements were made at frequencies near the resonant frequency of the nominal spring constant, and the resonant peak is fit to a Lorentzian peak function line. The spring constants obtained from the integration of the Lorentzian line by the Nanoscope software were 0.114 ± 0.008 N/m for the bare Si₃N₄ cantilevers, 0.127 ± 0.011 N/m for the gold-coated cantilevers, and 0.110 ± 0.006 N/m for the BSA-coated cantilevers. All three values have standard deviations of <10%. The spring constants of the cantilevers do not change significantly during our modification process. Therefore, our proposed method of covalent immobilization of proteins to AFM tips is a safe, easy, and nondestructive technique that can be used in a wide variety of protein-based studies.

Protein-Protein Interactions. The AFM was used to measure the adhesion forces between BSA immobilized on AFM cantilevers and either BSA or anti-BSA molecules immobilized on planar silicon wafers. Force measurements were performed in PBS buffer (pH 7.4). During AFM force measurements, the protein-coated cantilever is approached toward and then, after contact, retracted away from the planar substrate. The approach portion of the force curve represents the attraction or affinity a protein has for the surface based on long-range physiochemical interactions (e.g., hydrophobic or electrostatic). The retraction portion of the force curve represents the pull-off force or the force required to break short-range (van der Waals or hydrophobic) interactions or specific binding events.

During the approach of the BSA cantilever to either the BSA or the anti-BSA substrate, no long- or short-range attractive forces were detected by the AFM (data not shown). This is indicated by a smooth extension curve with no sudden jumps (reflecting an attractive interaction) or hyperextension (reflecting a repulsive interaction) of the cantilever. These results are consistent with the literature.²¹ Figure 3 shows representative curves of tip deflection versus the relative distance of separation for each protein combination during the retraction cycle of AFM force measurement. Retraction curves represent the pull-off force required to separate proteins after contact.

(17) Chen, G. Y.; Warmack, R. J.; Thundat, T.; Allison, D. P. *Rev. Sci. Instrum.* **1994**, *65*, 2532–2537.

(18) Cleveland, J. P.; Manne, S.; Bocek, D.; Hansma, P. K. *Rev. Sci. Instrum.* **1993**, *64*, 1–3.

(19) Hutter, J. L.; Bechhoefer, J. *Rev. Sci. Instrum.* **1993**, *64*, 1868–1873.

(20) Senden, T. J.; Ducker, W. A. *Langmuir* **1994**, *10*, 1003–1004.

(21) Kidoaki, S.; Matsuda, T. *Langmuir* **1999**, *15*, 7636–7646.

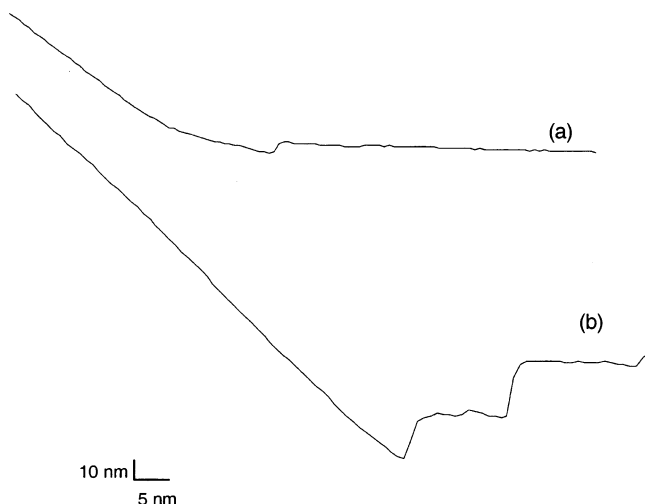


Figure 3. Representative curves of tip deflection during retraction vs the distance of separation between the BSA tips and (a) BSA and (b) anti-BSA surfaces during retraction.

Table 3. Average Pull-Off Forces between BSA tips and BSA or Anti-BSA Surfaces^a

surface	<i>n</i>	<i>F</i> (nN)	SD (nN)	<i>k</i> (N/m)
BSA	6	0.07	0.02	0.110 ± 0.006
anti-BSA	5	0.61	0.04	0.110 ± 0.006

^a *n* = number of freshly prepared tip/surface combinations, *F* = force, SD = standard deviation, *k* = spring constant.

The pull-off forces measured between BSA tips and BSA surfaces were very small, indicating little to no physicochemical interactions between BSA molecules (Table 3), which is consistent with previous research.²¹

The AFM was also used to measure the pull-off forces between BSA-coated tips and anti-BSA-coated surfaces. The corresponding pull-off force in Figure 3 appears "jagged" and actually represents the breaking of several antigen–antibody base pairs. This observation was consistent with similar AFM studies on antibody–antigen pairs.^{19–22} It is believed that, during contact, binding occurs between multiple BSA and anti-BSA antibody pairs.^{22–25} As seen in Figure 3, breaking of individual binding interactions occurs as discrete events during the retraction of the AFM cantilever. These discrete events have quantized numerical values representing the unbinding forces of individual molecular pairs.²⁶ Therefore, each discrete breaking force detected by the AFM represents the breaking of an individual or a group of receptor–ligand pairs. After analysis of numerous force curves, the magnitude of the pull-off force between BSA and anti-BSA was found to be 0.61 ± 0.04 nN (610 ± 40 pN). This value is consistent (to the same order of magnitude) with values found in the literature. For example, Hinterdorfer et al. reported the human serum albumin (HSA)/anti-HSA unbinding force to be 240 pN.^{27,28} Similarly, Lee et al. found the force between biotinylated BSA and strepta-

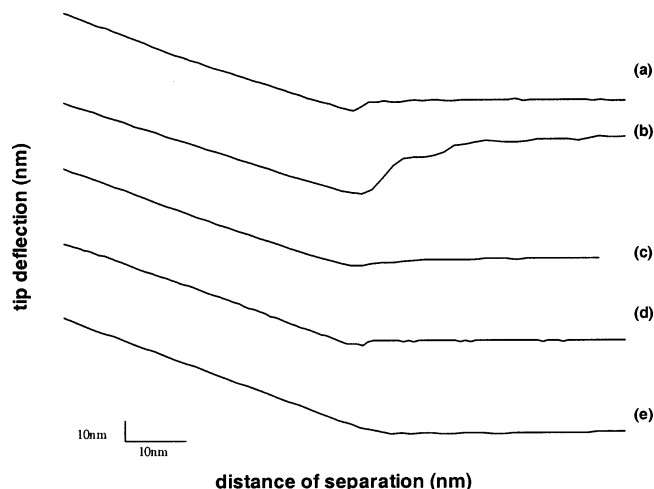


Figure 4. Representative curves of tip deflection vs the distance of separation curves between covalently immobilized BSA tips and (a) CH₃–, (b) OH–, (c) COOH–, and (d) NH₂ terminated SAMs.

Table 4. Average Pull-off Forces Measured between BSA Immobilized Tips and SAMs

surface	<i>n</i>	<i>F</i> (nN)	SD (nN)	<i>k</i> (N/m)
CH ₃	12	0.87	0.39	0.110 ± 0.006
OH	12	2.54	0.14	0.110 ± 0.006
COOH	9	0.98	0.30	0.110 ± 0.006
NH ₂	13	0.38	0.14	0.110 ± 0.006
dextran	4	0.09	0.04	0.110 ± 0.006

^a *n* = number of freshly prepared tip/surface combinations, *F* = force, SD = standard deviation, *k* = spring constant.

vidin to be 340 pN.²⁹ More importantly, the successful measurement of antibody–antigen binding interactions in this study demonstrates that both BSA and anti-BSA proteins retain their folded conformation and remain functional following our immobilization protocol.

Protein–Substrate and Protein–Dextran Interactions. AFM force measurements between the BSA-coated AFM cantilever and the various SAM or dextran substrates were carried out in PBS buffer. In all cases, no long- or short-range attractive forces were detected by the AFM during the approach cycle of the AFM force measurement (data not shown). This is indicated by the absence of sudden jumps or hyperextension of the cantilever as the protein-coated cantilever approached the substrate. Therefore, BSA protein did not have a strong propensity to bind to the SAM or dextran substrates from the buffer solution.

Conversely, the pull-off force measured during the retraction cycle represents the affinity of a protein for a surface after contact. Figure 4 depicts representative curves of tip deflection versus the relative distance of separation for BSA interacting with each substrate: SAMs with terminal functional groups of CH₃–, OH–, COOH–, NH₂–, and dextran. The adhesion forces calculated for each BSA/substrate combination are summarized in Table 4. The largest pull-off force and hence strength of adhesion was observed between the BSA and OH– terminated SAMs. The other three, CH₃–, COOH–, and NH₂– terminated SAMs, exhibited significant pull-off forces of equal magnitude. No pull-off force was detected between dextran and the BSA-coated cantilever.

(28) Hinterdorfer, P.; Kienberger, F.; Raab, A.; Gruber, H. J.; Baumgartner, W.; Kada, G.; Riener, C.; Wielert-Badt, S.; Borken, C.; Schindler, H. *Single Mol.* **2000**, *2*, 99–103.

(29) Lee, G. U.; Kidwell, D. A.; Colton, R. J. *Langmuir* **1994**, *10*, 354–357.

(22) Mulhern, P. J.; Blackford, B. L.; Jericho, M. H.; Southam, G.; Bereridge, T. J. *Ultramicroscopy* **1992**, 1214–1221.

(23) Ros, R.; Schwesinger, F.; Anselmetti, D.; Kubon, M.; Schäfer, R.; Plückthun, A.; Tiefenauer, L. *Proc. Natl. Acad. Sci. U.S.A.* **1998**, *95*, 7402–7405.

(24) Dammer, U.; Henger, M.; Anselmetti, D.; Wagner, P.; Dreier, M.; Huber, W.; Güntherodt, H. J. *Biophys. J.* **1996**, *70*, 2437–2441.

(25) Browning-Kelly, M. E.; Wadu-Mesthrige, K.; Hari, V.; Liu, G. Y. *Langmuir* **1997**, *13*, 343–350.

(26) Florin, E.-L.; Moy, V. T.; Gaub, H. E. *Science* **1994**, *264*, 415–417.

(27) Hinterdorfer, P.; Baumgartner, W.; Gruber, H. J.; Schilcher, H. J.; Schindler, H. *Proc. Natl. Acad. Sci. U.S.A.* **1996**, *93*, 3477–3481.

The interaction force measured between the BSA and CH₃ terminated SAMs was 0.87 ± 0.39 nN. This is in agreement with results from Rixman et al.³⁰ which report HSA-CH₃ terminated SAM interactions in the range from 0.79 to 1.88 nN. Conversely, Kidoaki et al. reported the BSA-CH₃ force of interaction as 4.5 ± 2.8 nN.²¹ However, the Kidoaki value is in agreement with the results of Rixman et al. because of the large standard deviation calculated in the Kidoaki study.²¹ Moreover, the forces measured in this study between albumin and COOH and NH₂ are consistent with both Kidoaki et al. and Rixman et al.³⁰ The major deviation between this work and previous studies is the large adhesive force detected between the BSA and OH terminated SAM.

Discussion

The goal of this study was to demonstrate that the AFM provides detailed information on protein adhesion to biomaterials that may be overlooked by traditional protein-adhesion techniques. Specifically, the AFM provides quantitative information on the magnitude of adhesion forces that can be used to guide the development of adhesion-resistant materials.

Successful detection of protein-protein interaction between BSA and anti-BSA molecules clearly demonstrates that the immobilization protocol employed herein does not alter the structure or function of the protein. BSA must have retained its structure to be recognized by the antibody, and the antibody must have retained its function to bind BSA. The immobilization protocol described in this work did not employ the flexible spacer molecules between the surface and the protein that have been used in previous immobilization techniques.²³ Previous studies employed long spacer molecules that were free to rotate to avoid surface effects on the protein.²³ The stretching or orientation of these spacer molecules, however, can introduce artifacts (such as conformational, steric, or bridging effects) into AFM force measurements. In this study, tightly packed SAMs representing a uniform interface were prepared directly on the tips of AFM cantilevers. Proteins were covalently attached to this interface. Since no adverse surface effects were detected on the proteins in this study, it can be argued that the freely rotating spacer molecules are not needed. Elimination of such spacer molecules makes for a cleaner system.

The AFM was used to measure the physiochemical interactions between BSA-coated tips and various SAM surfaces as well as dextran. These surface coatings represent potential modifications of biomaterial substrates for a solution to protein fouling and adverse physiological reactions. BSA protein was not attracted to any of these surfaces from solution during the approach cycles of the AFM force measurements. In other words, there were no long-range hydrophobic or electrostatic effects driving the proteins to the substrates. The substrates do not attract or act as a magnet for proteins in solution. Proteins probably arrive at the interface via simple diffusion and Brownian motion.

Conversely, during the retraction cycle, BSA protein displayed adhesive interactions with all the SAM substrates. Adhesion forces of equal magnitude were observed for hydrophobic CH₃- and hydrophilic COOH- and NH₂-terminated SAMs. The lack of strong adhesion between BSA and the hydrophobic CH₃- terminated SAMs indicates that hydrophobic interactions do not play a major role in BSA adhesion. Similarly, although the COOH-

and NH₂- terminated SAMs had the same contact angle, a larger interaction force was measured for COOH- in comparison to NH₂-. These results indicate that other forces in addition to hydrophobic interactions are involved in BSA adhesion (i.e., a specific binding interaction between BSA and the COOH- group). BSA is a small, hydrophilic protein that is not believed to interact strongly with biomaterials.³¹ Its compact structure and strongly hydrophilic surface explains why it is readily displaced by larger, more complex proteins during protein fouling of implants.^{2,31} The larger proteins may have more internal hydrophobic residues that become exposed during adhesion to surfaces.

Contrary to previous studies, the strongest adhesion force was measured between BSA and the OH- terminated SAMs. It is not believed that the OH- group forms a chemical bond with BSA; otherwise, breaking of multiple interactions would have been observed by the AFM, similar to the BSA/anti-BSA results. The contact angle measured on the OH terminated SAM was greater than those of the COOH and NH₂ terminated SAMs. In other words, the OH-SAM interface was more hydrophobic than expected. It is hypothesized that the OH- terminated SAMs may not have packed as tightly as the other SAMs evaluated in this study. If this were the case, then the BSA protein could be inserted into the hydrophobic (-CH₂-) backbone region of the SAM during AFM force measurements. Additional experiments are needed to understand the interactions of BSA with the OH- terminated SAMs as well as the OH-SAM packing in comparison to the other SAMs evaluated in this study.

In summary, our results contradict previous observations that hydrophobic surfaces promote protein adhesion but hydrophilic surfaces do not.¹ Surface hydrophobicity alone may not be the best indicator as to whether proteins will adhere. The chemistry, packing, or orientation of surface molecules in solution may also be involved. For example, surface coverage by the dextran may have been more extensive than the OH- terminated SAM, resulting in BSA adhesion to the OH- terminated SAM but not to dextran.

In similar studies, Sheth et al.³¹ used the surface force apparatus (SFA) to measure molecular forces between streptavidin and lipid bilayers displaying grafted poly(ethylene glycol) (PEG). SFA measurements demonstrate that the protein and PEG form relatively strong attractive forces, but these forces vary with the magnitude of the applied compressive forces. The forces were repulsive at low compressive loads, but they became attractive when the proteins were pressed into the polymer layer at higher loads. Sheth et al.³¹ suggested that this discrepancy could be attributed to the polydispersity of the polymer preparation or to an integral change in the PEG (such as induced or facilitated structural rearrangements in the polymer backbone). Furthermore, in their study, the polymer only interacted with a limited region of the protein surface. It was concluded that PEG was not always inert to protein adsorption depending on its state or conformation in water.³¹ Our work differs from the aforementioned study in that our system is not confined geometrically. The AFM allows van der Waals, electrostatic, and hydrophobic interactions to mediate protein-surface interactions as a function of the separation distance. AFM force measurements represent the *dynamic* interaction of proteins at interfaces. Nevertheless, results from this and the aforementioned SFA study demonstrate the potential uses

(30) Rixman, M. A.; Dean, D.; Macias, C. E.; Ortiz, C. *Langmuir* **2003**, *19*, 6202-6218.

(31) Sheth, S. R.; Leckband, D. *Proc. Natl. Acad. Sci. U.S.A.* **1997**, *94*, 8399-8404.

and pitfalls associated with using SAMs or polymers to modify biomaterial substrates. Moreover, both the SFA and the AFM provide the necessary information (force vs distance curves at the nanoscale level) to explore the effects of surface chemistry, packing, and orientation on adhesion.

As expected, no pull-off force was detected between the BSA-coated cantilever and dextran. The fact that dextran was the most hydrophilic surface alone does not explain its effectiveness at preventing protein adhesion. As discussed above, hydrophobic interactions were not a dominant force in BSA adhesion. The dextran molecules may be resisting protein adhesion by repulsive steric effects or hydration pressure. Repulsive steric effects arise due to an unfavorable rise in entropy associated with

compressing or confining polymers.³² Hydration pressure is due to short-range structural forces that usually appear at separation distances ≤ 4 nm;^{33–35} however, they have been observed at separations of 10 nm or more.³⁶ While the origin and nature of hydration pressure is not completely understood, it appears to arise whenever water molecules bind to strongly hydrophilic materials. In summary, dextran represents a promising surface modification strategy for eliminating nonspecific adhesion of proteins at biomaterial interfaces.

Acknowledgment. This research was supported by the donors of the Petroleum Research Fund, administered by the American Chemical Society, and the Whitaker Foundation Biomedical Engineering Research Grant Program. Thanks also to Professor Steven Massia and Dr. Gholam Ehteshami at the Harrington Department of Bioengineering at Arizona State University for preparing the dextran-coated surfaces.

LA049849+

(32) Israelachvili, J. *Intermolecular and Surface Forces*, 2nd ed.; Academic Press Limited: San Diego, CA, 1992.

(33) Pashley, R. J. *J. Colloid Interface Sci.* **1980**, *80*, 153–162.

(34) Pashley, R. M. *J. Colloid Interface Sci.* **1981**, *83*, 531–546.

(35) Basu, S.; Sharma, M. M. *J. Colloid Interface Sci.* **1996**, *181*, 443–455.

(36) Ninham, B. *Adv. Colloid Interface Sci.* **1999**, *83*, 1–17.